Dynamic nodes, edges, and subnetworks in brain connectivity

Alice Misun Yoon

Department of Medical Science

The Graduate School, Yonsei University

Dynamic nodes, edges, and subnetworks in brain connectivity

Directed by Professor Hae-Jeong Park

The Master's Thesis
submitted to the Department of Medical Science,
the Graduate School of Yonsei University
in partial fulfillment of the requirements for the degree
of Master of Medical Science

Alice Misun Yoon

December 2014

This certifies that the Master's Thesis
Of Alice Misun Yoon is approved.

Thesis Supervisor: Hae-Jeong Park

Thesis Committee Member#1: Jong Doo Lee

Thesis Committee Member#2: Sangwoo Kim

The Graduate School
Yonsei University

December 2014

ACKNOWLEDGEMENTS

It is my great pleasure to acknowledge everyone who has supported me in the successful completion of my thesis. This thesis would not have been possible without much guidance and help from these people.

First and foremost, I would like to express my sincere gratitude to my advisor, Professor Hae-Jeong Park for the continuous support of my master's study and research with his patience, motivation, enthusiasm and immense knowledge. With his guidance and insight, I was able to come up with this thesis topic, research and write this thesis.

My thesis committee guided me with insightful comments and valuable encouragement. I wish to thank Professor Jong Doo Lee, for his unstinting support of my graduate studies as former dean of the department. He led my research in a consistent direction and drew the big picture for my work. Thanks to Professor Sangwoo Kim for critical advice that contributed to successfully completing my thesis. I have been deeply honored to have these faculty as members of my thesis committee.

I am grateful to colleagues in the MoNET lab for their various support and help. I would like to begin by thanking Mr. Maeng-Keun Oh for the preprocessing and management of data. I would also like to thank Dr. Bumhee Park for his generous guidance, which helped me grow tremendously in this field. My thanks go to Shin-ae Yoon, who was always there for me and

encouraged me sincerely. Dr. Dongha Lee was the perfect example to me of an enthusiastic neuroscientist. Thanks to Chongwon Pae, who assisted me with his talents and gave me a ride home from time to time. Thanks to Changwon Jang for valuable conversation on diverse topics. Thanks to Cao Tri Do, who was my great partner with keen insight. I also would like to thank So Mang Kang, Jae-Chang Kim, Sunghyon Kyeong and Jinseong Kim, who supported me in many ways.

Finally, I would like to thank my family for their unwavering support and love. I especially appreciate my grandmother, who has taken care of me all my life. I am thankful my parents, sister and brother for their support and trust.

TABLE OF CONTENTS

ABSTRACT 1

I. INTRODUCTION 3

II. MATERIALS AND METHODS 7

1. Subjects 7
2. MR Acquisition 7
3. Image preprocessing 9
4. Functional brain networks 9
   A. Node definition 9
   B. Signal Processing 9
   C. Construction of functional connectivity 10
5. Multilayer modularity optimization and nodal entropy 10
6. Intra-class correlation 13
7. Effective brain networks 14
   A. Dynamic Causal Modelling (DCM) 14
   B. Stochastic DCM 15
   C. Defining the functional module 15
      (1) Modularity optimization 16
   D. Consistency in within-module effective connectivity 16

III. RESULTS 18

1. Dynamic nodes in the functional brain network 18
   A. Temporal variation of node properties 18
   B. Entropy of nodes from multilayer modularity optimization 19
2. Dynamic edges in the functional brain network 21
3. Dynamic subnetworks in the functional brain network 21

A. Temporal variation in graph ICA components' usage-strength 21
4. Dynamicity in effective brain connectivity 23
A. Defined Module 23
B. The dynamics of intra-module effective connectivity in lower le
vel area and higher cognitive frontal area 26
IV. DISCUSSION 27
1. Characteristics of dynamic nodes 28
2. Characters of dynamic and stable edges 30
3. Features of dynamic subnetworks 30
V. CONCLUSION 32
REFERENCES 33
ABSTRACT (IN KOREAN) 40

LIST OF FIGURES

Figure 1. Concept of dynamic node, edge, and subnetwork 4
Figure 2. Problem of stochastic DCM for whole brain effective networks 6
Figure 3. Resting-state fMRI acquisition during 24 hours..... 8
Figure 4. Rand coefficient: Similarity between partitionings fr om modularity optimizations 12
Figure 5. Entropy(complexitiy) in multilayer modularity optim ization..... 13
Figure 6. Consistency in within module effective connectivity 17
Figure 7. Dynamic nodes according to topological properties 18
Figure 8. Entropy of nodes with multilayer modularity optimiz ation..... 19
Figure 9. Dynamic edges; ICC of functional connection weight s 21
Figure 10. Dynamic subnetworks with graph ICA components usage-strength 22
Figure 11. Functional module definition by modularity optimiz ation..... 23
Figure 12. Consistency map of 38 modules..... 25

Figure 13. Comparison dynamicity between lower sensory are a and high order frontal area 26

LIST OF TABLES

Table 1. Nodes with high entropy and entropy values..... 20
Table 2. Functional modules and names of nodes 23

ABSTRACT

Dynamic nodes, edges, and subnetworks in brain connectivity

Alice Misun Yoon

Department of Medical Science
The Graduate School, Yonsei University

(Directed by Professor Hae-Jeong Park)

Recent brain research has been expedited by the network brain theory and neuroimaging methods for constructing whole-brain structural and functional brain networks. Functional brain networks are constructed based on the synchronous fMRI signal fluctuations among brain regions during resting state. Numerous studies have utilized functional brain network analysis to characterize individuals, to understand diseases and to test effects of treatments. All these applications of resting state functional brain networks were based on the assumption that functional brain networks are sufficiently stationary enough to describe a relatively long-lasting brain state. However, recent studies have shown dynamic natures of resting state brain networks within a relatively short time period. Thus, this study investigates dynamicity of network nodes, edges, and subnetworks of the whole brain using repeatedly measured fMRI data. We particularly focused on the hypothesis that integration among subregions of each node is highly dynamic, i.e., dynamic heterogeneity among voxels within a node. We also hypothesized that brain regions for highly dynamic membership

for whole brain modules (high entropy) may correspond to hub regions. To test this hypothesis, we used resting state fMRI data from 12 healthy subjects measured at eight sessions during a 24-hour period. To evaluate the dynamicity of nodes, edges and other network properties, we used intra-class correlation (ICC). We found that highly stable node strength, node efficiency and clustering coefficient (ICC>0.5) at the bilateral superior parietal gyri, right precuneus, left hippocampus, and lateral inferior parietal lobule. We also found high entropy at bilateral parahippocampal gyri, bilateral hippocampus, and bilateral superior frontal gyri. These regions overlap with rich-club brain areas in previous studies. When we measured principal component analysis of each ROI time series, highly heterogeneous integration within ROI were found especially higher order brain regions. Furthermore, we examined the temporal consistency of effective connectivity of brain network submodules by looking at correlation between eight sessions. The higher order frontal area showed more dynamicity than lower sensory areas such as primary visual and auditory cortices.

All these results reveal dynamic natures of the brain even during a 24-hour period. These dynamicity is not only node properties, edge strengths but also within node heterogeneous integrations, membership complexities and effective connectivities.

Key words: functional magnetic resonance imaging; brain connectome; resting state functional connectivity; graph theory; brain subnetwork; dynamic components;

Dynamic nodes, edges, and subnetworks in brain connectivity

Alice Misun Yoon

Department of Medical Science
The Graduate School, Yonsei University

(Directed by Professor Hae-Jeong Park)

I. INTRODUCTION

The human brain consists of one hundred billion neurons that are interconnected to form a relatively small number of functional neural networks enabling human behavior and cognition. Moreover, the brain shows flexibility in regional activity and large-scale circuits when someone learns a new skill, and resilience through reorganization after brain damage (e.g., stroke or Parkinson's disease). To explain these dynamic properties of a fixed structure, scientists have recently focused on functional brain networks. The spontaneous activity of networks during the resting state is used to identify connectional changes in the brain. It has been employed in various studies such as in blind, depressed patients[1, 2] and has been used to evaluate the level of the consciousness during sleep state[3].

Despite a large number of studies on brain networks, researches on their dynamicity or stability is still lacking. In particular, which parts of brain networks remain stable or dynamic over the course of a day remains to be

explored. The time of day has been reported to influence cognition in executive functioning, attention, and working memory[4-6]. Furthermore, previous fMRI studies have demonstrated changes in brain activation[7] between night and afternoon and a stable brain network over 24 hours[8]. These studies raise further questions regarding the dynamic elements of resting state functional connectivity over the course of a day.

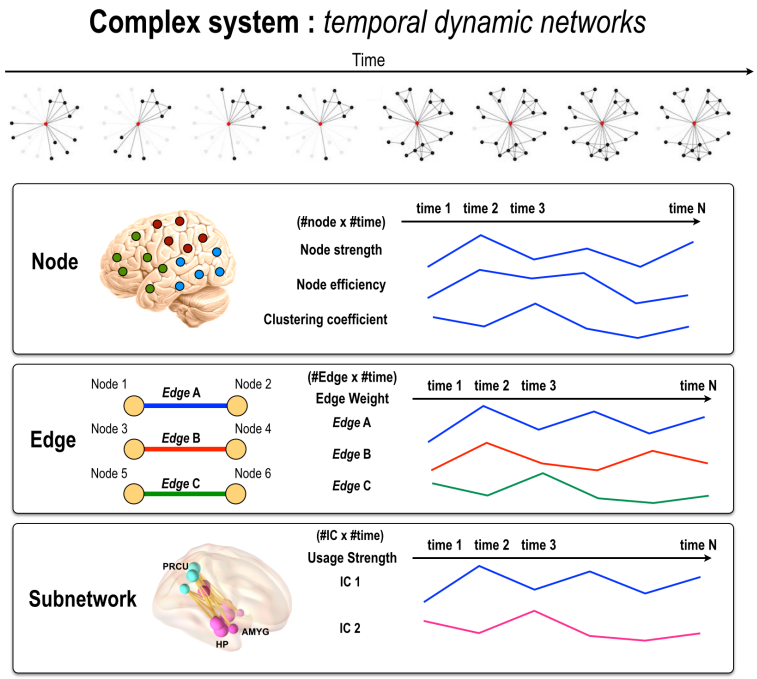

Figure 1. Concept of dynamic node, edge, and subnetwork

The current study thus focuses on the following questions: What nodes, edges, and subnetworks display dynamicity over 24 hours? How can we

identify them in a functional brain network? (Figure 1) We found dynamic nodes with the topological properties of nodes in the functional brain network. The synchronization between two nodes, called an “edge” was also investigated to find dynamic synchronicities in brain. Moreover, in this study, we emphasized the human brain’s in hierarchical structure, which consists of several functional subnetworks. Within such subnetworks, hubs exist to connect different nodes, resulting in small-world and scale-free properties[9-12]. Recent findings on human brain networks provide ample evidence that some brain regions may serve as hubs that are not responsible for only a single function but are engaged in multiple cognitive functions. Thus, we also looked at dynamic subnetworks to understand diverse brain functions.

Since the brain is a complex system, the brain system’s dynamics should be measured over time and explained as a dynamic model[13-15]. In this study, therefore, the dynamicity of effective brain connectivity was estimated by stochastic DCM, which considers random fluctuations in resting state dynamic connectivity in the brain[16, 17]. Based on the assumption that the brain function is determined by its functional segregation as the local level and integration as a whole, we overcame the problems (Figure 2) of estimating of whole brain effective connectivity by using the module separation approach.

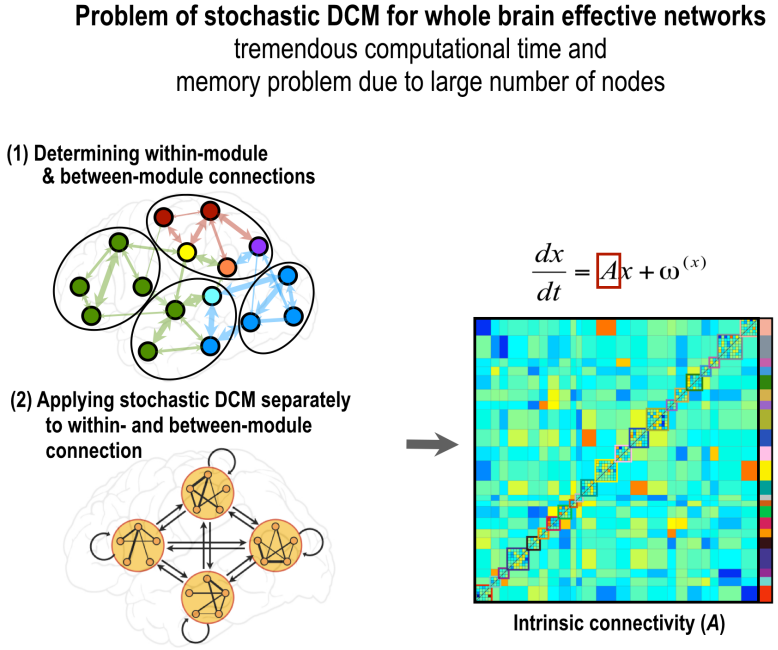

Figure 2. Problem of stochastic DCM for whole brain effective networks

Stochastic DCM has limitations in calculating large-scale connectivity, since current stochastic DCM is optimized for small-scale connectivity. This leads to infeasible computational time and memory shortage. Thus, we introduced a novel method that uses stochastic DCM to estimate large-scale brain connectivity using modules of the whole brain.

II. MATERIALS AND METHODS

1. Subjects

This study included two independent groups of subjects for each purpose. To examine brain network dynamics, twelve healthy and right-handed participants (nine males and three females, mean age 25.42 ± 2.84 years) were recruited for the study. Another group of 234 healthy and right-handed subjects (115 males and 119 females, mean age 24.53 ± 7.69 years) were also included for defining functional network nodes. Handedness was assessed using a Korean version of the Annett handedness questionnaire[18]. None of the participants had a history of neurological illness, sleep problems, or psychiatric disorders. This study followed the human subject guidelines approved by the Institutional Review Board of the Yonsei University College of Medicine, and all participants gave informed consent before MRI examinations.

2. MR Acquisition

All subjects underwent fMRI scanning with a 3.0 Tesla MRI scanner (Siemens Tim Trio, Erlangen, Germany) to obtain T2* weighted single shot echo planar imaging (EPI) sequences. Each subject was scanned axially using the following parameters: voxel size, 3.0×3.0×3.3 mm^3; slice number, 32 (interleaved); matrix, 64×64; slice thickness, 3.3 mm; repetition time (TR), 2000 ms; echo time (TE), 30 ms; and field of view, 192 mm. Each 330-sec scan

produced 165 fMRI images, which is known to be sufficient to evaluate resting state functional connectivity and to obtain low frequency oscillation for the resting state functional connectivity.

To facilitate later spatial normalization, a high-resolution structural data set was also obtained from each subject using a magnetization-prepared rapid acquisition gradient echo (MP-RAGE) three-dimensional T1-weighted sequence (voxel size, 0.9×0.9×1.0 mm^3; TR, 2300 ms; TE, 3.08 ms). Foam pads were used to reduce head motion during EPI data acquisition. Each subject was scanned for 10 min, while resting with eyes closed, for eight sessions at different times-of-day: 19:00 (1^{st} day), 21:00, 1:00 (2^{nd} day), 7:00, 10:00, 13:00, 16:00, and 19:00 (Figure 3). We did not scan subjects at 3:00 am (2^{nd} day) in order not to disturb normal sleep. For each scan, subjects were instructed to keep their eyes closed, without sleeping or specific thinking. After scanning, subjects were asked to report their sleepiness and general condition.

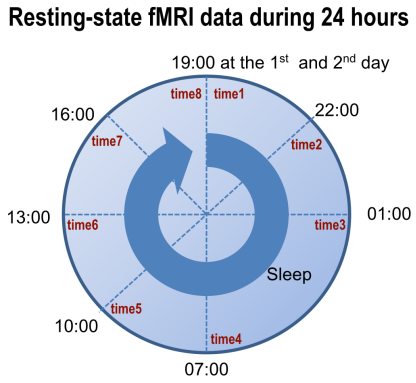

Figure 3. Resting-state fMRI acquisition during 24 hours

3. Image preprocessing

Image preprocessing was conducted using statistical parametric mapping (SPM8, Wellcome Department of Cognitive Neurology, London, UK)[19]. After discarding the first 5 scans for stability issues, the 160 EPI data were preprocessed by correction of the acquisition time delay between different slices, and correction for head motion by realignment of all consecutive volumes to the first image of the session. The realigned images were co-registered to T1-weighted images, which were used to spatially normalize functional data into a template space using nonlinear transformation.

4. Functional brain networks

A. Node definition

To construct individual functional networks, we used two maps: an automated anatomical labeling (AAL) map[20] and a map produced through anatomy-constrained hierarchical modularity optimization (AHMO)[21] to AAL (AAL-AHMO). We broke up the AAL's 121 regions into a functionally more homogeneous set of 424 regions, and we applied the AHMO to a dataset of 234 subjects.

B. Signal Processing

FMRI time courses were processed using band-pass filtering (0.009–0.1Hz)

and by regressing out effects of rigid motion and their derivatives and global signal changes in the whole brain[22-24]. We also regressed out the top three principal components of white matter and cerebrospinal fluid[25]. To deal with the head motion effect that is often an issue in functional network analysis [26-28], we added derivatives of the motion parameters as covariates[26].

C. Construction of functional connectivity

To obtain individual whole brain networks, we calculated an interregional correlation map (adjacency matrix) for each mean fMRI time series among the 121 and 424 regions. For total of 8 acquisition times for 12 subjects, correlation coefficients between the mean time series of the two sets of regions were calculated. We transformed the correlation coefficients into z-scores using Fisher's r-to-z transformation and thresholded each individual set using false positive rate (FDR) < 0.05 [29]. For individual functional networks, we calculated global/local efficiency and nodal degree/strength[30].

5. Multilayer modularity optimization and nodal entropy

To investigate the dynamic modular organization of the functional brain network, we adopted a multilayer modularity optimization[31], in which each layer (time) network represents a functional network at each acquisition time point over the course of a day. Multilayer modularity optimization for each

subject was calculated as the following:

$$Q_{ml} = \frac{1}{2\mu}\sum_{ijlr}\left\{\left(A_{ijl} - \gamma_l \frac{k_{il}k_{jl}}{2m_l}\right)\delta_{lr} + \delta_{ij}C_{jlr}\right\}\delta(g_{il}, g_{ir})\delta_{lr}$$

where the adjacency matrix of layer l has connection elements A_{ijl}; γ_i is the resolution parameter of layer l, which was set to 1 for all layers; g_{jr} is the community membership of node j in layer r; C_{ilr} is the connection weight between node j in layer r and node j in layer l with constant C = 1; k_{il} is the strength of node i in layer l, $2\mu = \sum_{jr} k_{jr}$, $k_{jr} = k_{jl} + c_{jl}$, $c_{jl} = \sum_r c_{jlr}$; and δ=1 if they are assigned to same community, otherwise δ=0.

Since the multilayer modularity optimization algorithm can detect different partitioning run by run, we selected one representative community structure after running the community detection algorithm 100 times using a similarity measure (Figure 4), the z-score of the Rand coefficient, defined as follows[32, 33]:

$$S_R = \frac{\omega_{11} - \frac{1}{M}(\omega_{11} + \omega_{10})(\omega_{11} + \omega_{01})}{\frac{1}{2}[(\omega_{11} + \omega_{10}) + (\omega_{11} + \omega_{01})] - \frac{1}{M}(\omega_{11} + \omega_{10})(\omega_{11} + \omega_{01})}$$

where M is the number of all possible pairs, $M_1 = \sum_i \binom{n_{i\cdot}}{2}$ is the number of pairs in the first partition, and the equivalent quantity for the second partition is $M_2 = \sum_j \binom{n_{\cdot j}}{2}$, using $n_{i\cdot} = \sum_j n_{ij}$, $n_{\cdot j} = \sum_i n_{ij}$, $\omega := \omega_{11} = \sum_{ij}\binom{n_{ij}}{2}$, $\omega_{10} = M_1 - \omega$, $\omega_{01} = M_2 - \omega$, and $\omega_{00} = M - M_1 - M_2 + \omega$. The z-score of the Rand coefficient is known to follow from standardized normal distribution[32, 33].

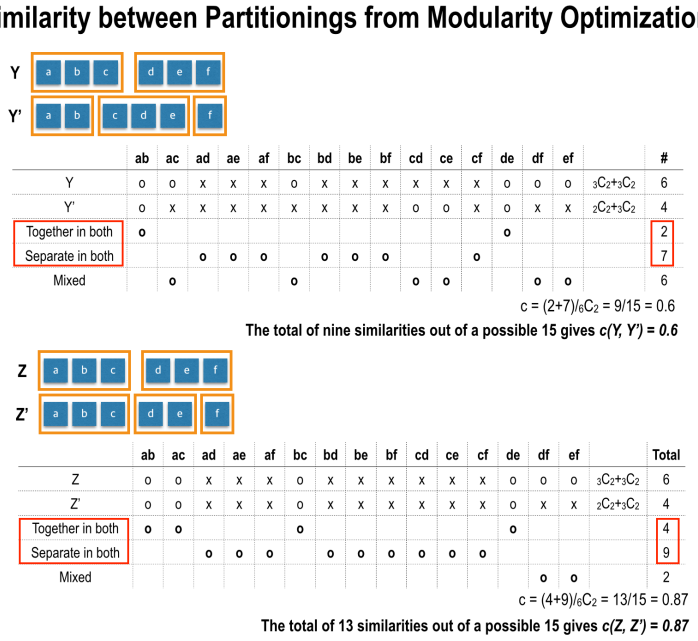

Figure 4. Rand coefficient: Similarity between partitionings from modularity optimizations

After calculating the z-score of the Rand coefficient for all possible pairs, we automatically selected representative modular partitioning showing the highest sum of similarities. The z-score of the Rand coefficient was also used to assess the similarity among modular partitionings at different acquisition times.

In addition, to measure the temporal variability of the modular structure and entropy of each node (Figure 5), E_i was calculated, which was defined as the complexity of community assignment through the number of modules and number of members in each module.

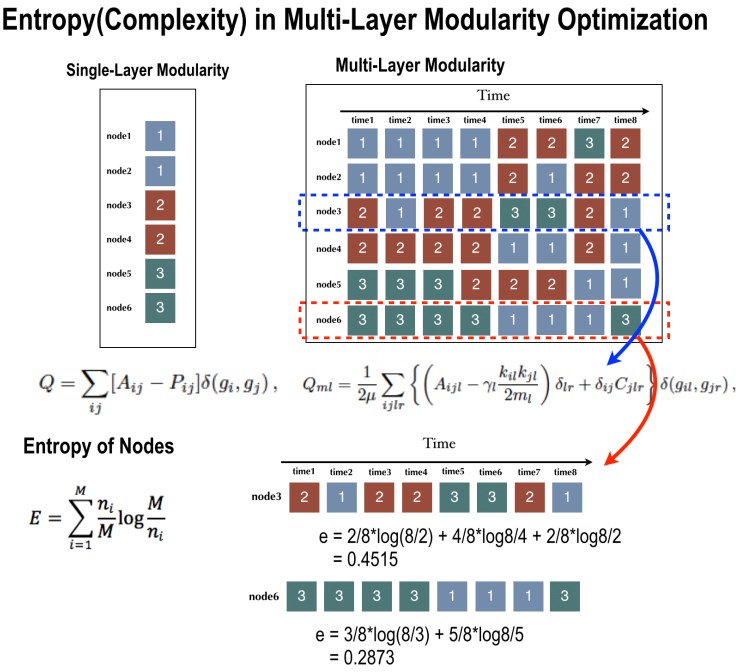

Figure 5. Entropy(complexitiy) in multilayer modularity optimization

6. Intra-class correlation

We used intra-class correlation (ICC)[34-36] to test the dynamicity of each of the metrics described in the previous sections. ICC was calculated using two variances in a two-way mixed effect model[34] such as

$$ICC = \frac{\sigma_\alpha^2}{\sigma_\alpha^2 + \sigma_e^2} = \frac{MSB - MSE}{MSB + (k-1)MSE}$$

where σ_α^2 and σ_e^2 are between- and within-subject variance, *MSB* and *MSE* represent mean squares of between- and within-subject factors, and *k* represents the number of sessions. We interpreted the ICC values using empirical criteria

taken from previous studies[36, 37], which regarded ICC as poor for ICC < 0.4; fair for 0.4 ≤ ICC < 0.5; or good for ICC ≥ 0.5.

7. Effective brain networks

A. Dynamic Causal Modelling (DCM)

To infer the causal effects of dynamic systems with directionality, we used dynamic causal modeling (DCM)[14]. DCM is a Bayesian model comparison procedure that compares how the observed data were generated. Dynamic causal models are formulated in terms of ordinary differential equations (i.e., nonlinear state-space models in continuous time). These equations model the dynamics of hidden states in the nodes, where conditional dependencies are parameterized in terms of directed effective connectivity[14]. Compared to Bayesian networks the graphs used in DCM can be cyclic. Moreover, different from structural equation modeling (SEM) and Granger causality, DCM does not depend on the Martingale's theory[38], and thus does not assume that random fluctuations' are serially uncorrelated[13]. DCM for fMRI uses a deterministic model of neural dynamics in a network or graph of *n* interacting brain regions or nodes[14, 15]. It models the changes of a neuronal state-vector *x* in time, where each region is represented by a single hidden state using the following bilinear differential equation:

$$\dot{x} = f(x, u, \theta) = Ax + \sum_{j=1}^{m} u_j B^{(j)} x + Cu$$

B. Stochastic DCM

Stochastic DCM differs from conventional deterministic DCM by allowing for endogenous or random fluctuations in unobserved (hidden) neuronal and physiological states, known technically as system or state noise[16, 17].

$$\dot{x} = Ax + \sum_{j=1}^{m} u_j B^{(j)} x + Cv + \omega^{(x)}$$

$$v = u + \omega^{(x)}$$

Finally, the opportunity to model endogenous fluctuations means that one can, in principle, identify the functional architectures (effective connectivity) underlying the endogenous dynamics observed in resting-state studies.

C. Defining the functional module

A problem was encountered in the estimation of the whole brain effective network using stochastic DCM: tremendous computational time and memory was used for inversion due to a large number of nodes. To address this problem, we applied stochastic DCM separately to submodular areas defined from the whole brain.

Prior to modularity optimization, we conducted Fisher's r-to-z

transformation for inter-regional functional connectivity among 424 cortical regions for each subject and averaged them. We used network-forming initial threshold with $p<0.001$.

(1) Modularity optimization

Modularity (Q) is defined as (total connection weight within subnetwork) – (chance-expected total connection weight) and modularity optimization is used to find network-partitioning maximizing Q[39, 40]. This mathematical concept is expressed as follows[39, 40]:

$$Q = \frac{1}{V}\sum_{ij}(w_{ij} - e_{ij})\delta_{M_iM_j}$$

$$e_{ij} = \frac{s_i s_j}{V}, s_i = \sum_j w_{ij}, V = \sum_{ij} w_{ij}$$

where e_{ij} is chance-expected total weight; w_{ij} is connection weight between node i and j; V is total sum of weights, rescaling Q to [0,1]; and $\delta_{M_iM_j}$ is an indicator that becomes one if node i and j are in the same subnetwork and zero otherwise.

D. Consistency in within-module effective connectivity

To measure the temporal consistency using 8 acquired effective connectivites per subject for each module, we examined correlation among time points. We obtained 24 consistency measures for each subject and each module by calculating all possible combinations of 8 time points (Figure 6).

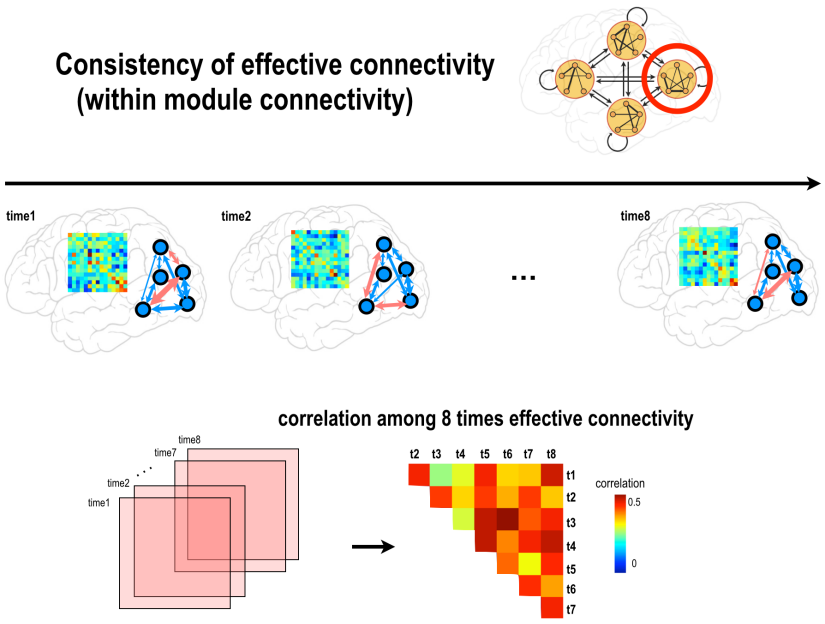

Figure 6. Consistency in within module effective connectivity

III. RESULTS

1. Dynamic nodes in the functional brain network

A. Temporal variation of node properties

Local graph metrics such as node strength, node efficiency, and clustering coefficient showed large dynamics (ICC<0.4), although we found stable (ICC≥0.5) nodal strength in specific locations including the bilateral middle temporal gyri, right insular gyrus, and right superior temporal gyrus, and right superior orbital frontal gyrus. The clustering coefficient was stable in parts of right nucleus accumbens (ICC=0.50) and right hippocampus (ICC=0.51) (Figure 7).

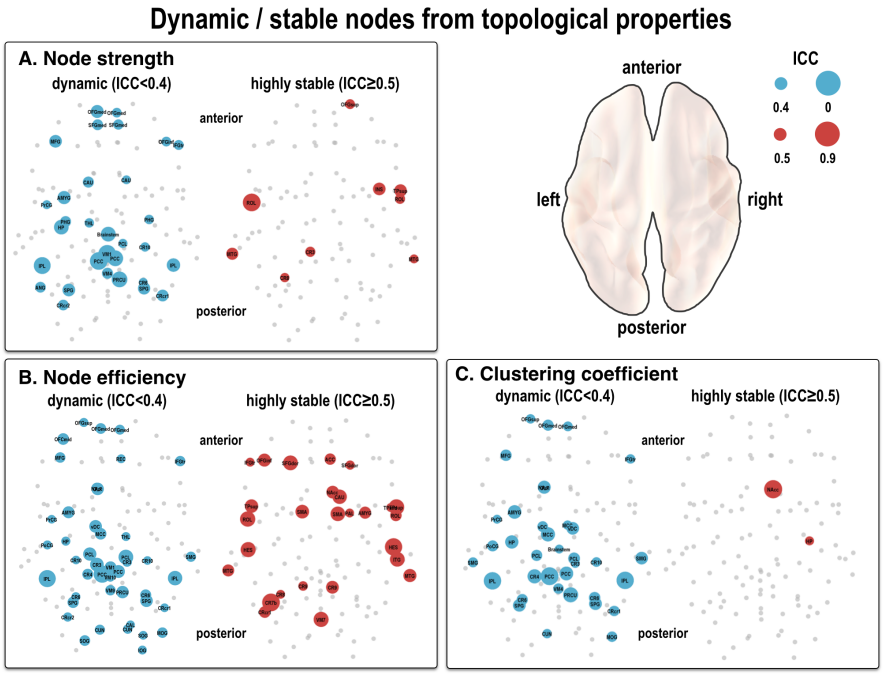

Figure 7. Dynamic nodes according to topological properties

B. Entropy of nodes from multilayer modularity optimization

Multilayer modularity optimization identified the modular structure separately for each subject at each acquisition time point. We found significant values of nodal entropy (i.e., the complexity of nodal modular membership assignments) in subcortical regions, including the left caudate, left nucleus accumbens, bilateral parahippocampal gyri, bilateral hippocampus, and amygdala, as well as in cortical regions such as the bilateral posterior cingulate cortex, temporal pole, middle temporal gyrus, right precentral gyrus, postcentral gyrus, bilateral anterior cingulate gyrus, left frontal pole, bilateral temporal pole, posterior parts of the bilateral superior and inferior temporal gyri (FDR<0.05 in one sample *t*-test) (Table 1, Figure 8).

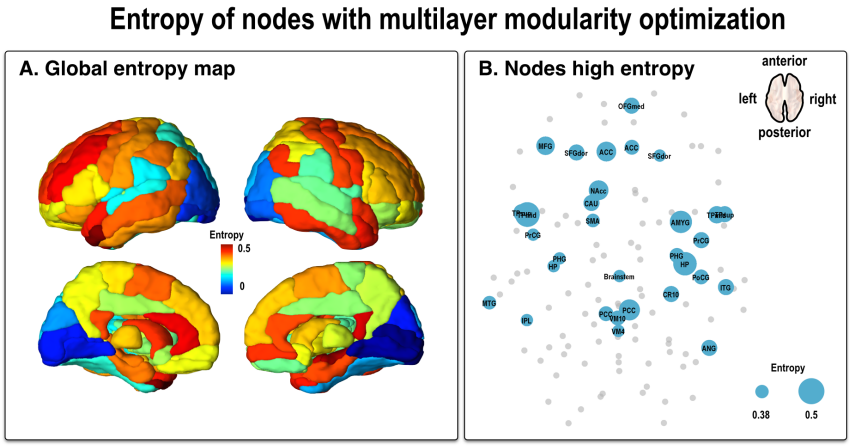

Figure 8. Entropy of nodes with multilayer modularity optimization

Table 1. Nodes with high entropy and entropy values

Node Name	Abbreviation	Entropy
Temporal pole, middle temporal gyrus left	TPmid.L	0.4659
Hippocampus right	HP.R	0.4641
Amygdala right	AMYG.R	0.4601
Posterior cingulate gyrus right	PCC.R	0.4554
Nucleus accumbens left	NAcc.L	0.4490
Anterior cingulate gyrus left	ACC.L	0.4469
Middle frontal gyrus left	MFG.L	0.4385
Temporal pole, superior temporal gyrus left	TPsup.L	0.4210
Temporal pole, middle temporal gyrus right	TPmid.R	0.4168
Angular gyrus right	ANG.R	0.4104
Cuadate nucleus left	CAU.L	0.4101
Precentral gyrus right	PrCG.R	0.4065
Superior frontal gyrus, dorsolateral left	SFGdor.L	0.4002
Superior frontal gyrus, medial orbital	OFGmed.R	0.3896
Temporal pole, superior temporal gyrus right	TPsup.R	0.3883
Inferior temporal gyrus right	ITG.R	0.3857
Anterior cingulate gyrus right	ACC.R	0.3813
Posterior cingulate gyrus left	PCC.L	0.3811
Parahippocampal gyrus right	PHG.R	0.3808
Olfactory cortex left	PoCG.R	0.3794
Supplementary motor area left	SMA.L	0.3785
Middle temporal gyrus left	MTG.L	0.3780

2. Dynamic edges in the functional brain network

We found that all regions displayed dynamic resting-state functional connectivity (ICC < 0.4; density = 94.4 %), as well as connectivity that was highly stable (ICC ≥ 0.5; density = 0.6 %) and fairly stable (0.4 ≤ ICC < 0.5; density = 5 %) (Figure 9).

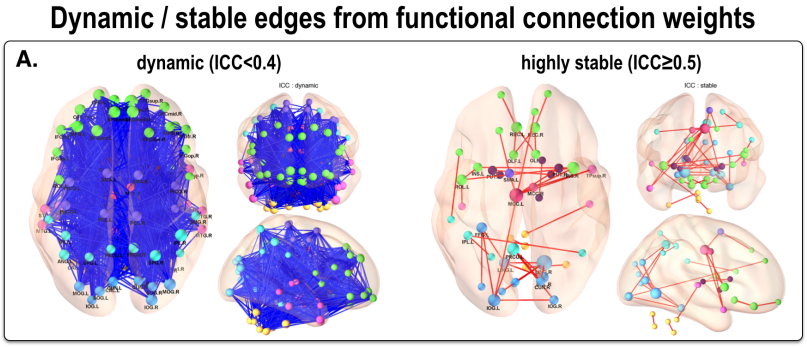

Figure 9. Dynamic edges; ICC of functional connection weights

3. Dynamic subnetworks in the functional brain network

A. Temporal variation in graph ICA components' usage-strength

Usage strength for graph ICA components provided the measurement of subnetwork usage for each session. We obtained 67 ICA components and found no stable ICA components (ICC ≥ 0.4) among them. We examined four components with low ICC values. IC2 (ICC=0.24) and IC41 (ICC=0.38) showed subnetworks consisting of bilateral superior frontal gyri (dorsolateral, orbital part, and medial), bilateral middle frontal gyri, and bilateral inferior

frontal gyri. IC64 (ICC=0.14), where the orbital part of the superior frontal gyrus was mainly connected with the occipital lobe, had the lowest ICC value. IC12 (ICC=0.33) included subcortical regions with the bilateral thalamus, bilateral parahippocampal gyri, bilateral hippocampus, and bilateral amygdala, as well as cortical regions including the bilateral precuneus and cerebellum (Figure 10).

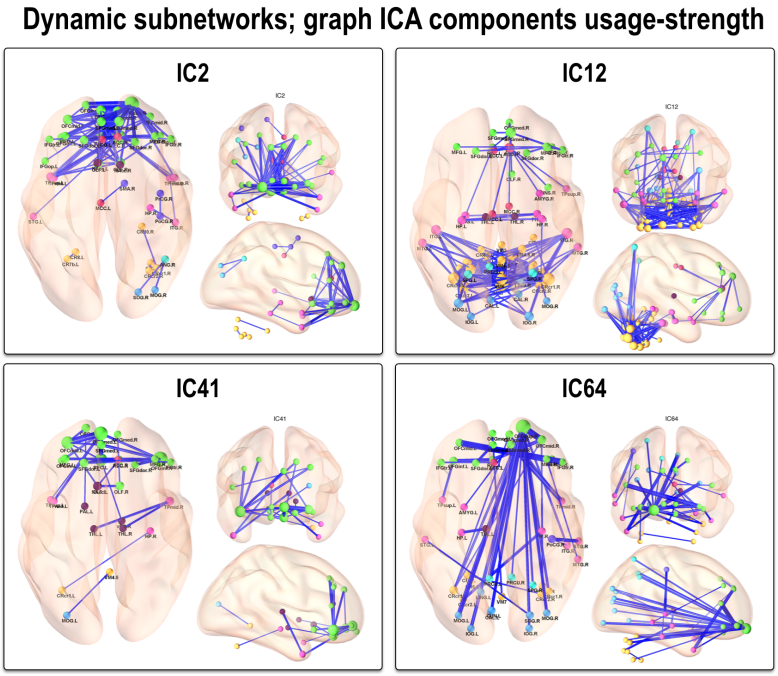

Figure 10. Dynamic subnetworks with graph ICA components usage-strength

4. Dynamicity in effective brain connectivity

A. Defined Module

Thirty-eight subnetworks of whole brain were defined using the modularity optimization algorithm from AAL-AHMO, which has 424 nodes (Table 2, Figure 11). The number of nodes in each module ranged from 6 to 18.

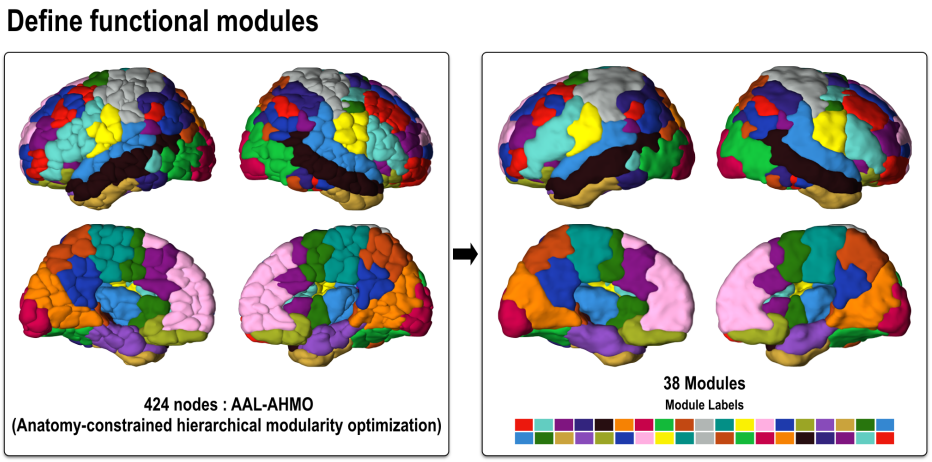

Figure 11. Functional module definition by modularity optimization

Table 2. Functional modules and names of nodes

Module	Nodes	Abbreviation
Module5	Temporal pole, superior temporal gyrus.2	TPsup.2.L
	Middle temporal gyrus.1-14	MTG.1.L
		MTG.2.L
		MTG.3.L
		MTG.4.L
		MTG.5.L
	Temporal pole, middle temporal gyrus.2	MTG.7.L
		MTG.8.L

		MTG.9.L
		MTG.11.L
		MTG.12.L
		MTG.13.L
		MTG.14.L
		TPmid.2.L
Module 7	Calcarine fissure and surrounding cortex.1-2	CAL.1.L
		CAL.2.L
	Lingual gyrus.1-2	LING.1.L
		LING.2.L
	Superior occipital gyrus.1-2	SOG.1.L
		SOG.2.L
	Middle occipital gyrus.2	MOG.2.L
	Inferior occipital gyrus.3	IOG.3.L
Module 11	Supplementary motor area.2, 4	SMA.2.L
		SMA.4.L
	Median cingulate and paracingulate gyri.2, 4	MCC.2.L
		MCC.4.L
	Paracentral lobule. 1-4	PCL.1.L
		PCL.2.L
		PCL.3.L
		PCL.4.L
Module 13	Superior frontal gyrus, dorsolateral.2	SFGdor.2.L
	Supplementary motor area.6	SMA.6.L
	Superior frontal gyrus, medial.1-7	SFGmed.1.L
		SFGmed.2.L
		SFGmed.3.L
		SFGmed.4.L
		SFGmed.5.L
		SFGmed.6.L
		SFGmed.7.L
	Superior frontal gyrus, medial orbital.1-2	OFGmed.1.L
		OFGmed.2.L
	Anterior cingulate and paracingulate gyri.1-3	ACC.1.L
		ACC.2.L

		ACC.3.L
Module 14	Superior frontal gyrus, dorsolateral.1, 3-5,7	SFGdor.1.L
		SFGdor.3.L
		SFGdor.4.L
		SFGdor.5.L
		SFGdor.7.L
	Superior frontal gyrus, orbital part.3	OFGsup.3.L
	Middle frontal gyrus.4-5, 11	MFG.4.L
		MFG.5.L
		MFG.11.L
	Median cingulate and paracingulate gyri.3	MCC.3.L
	Posterior cingulate gyrus.1	PCC.1.L
	Angular gyrus.1-3	ANG.1.L
		ANG.2.L
		ANG.3.L
	Precuneus.1-2, 3, 6	PRCU.1.L
		PRCU.2.L
		PRCU.3.L
		PRCU.6.L

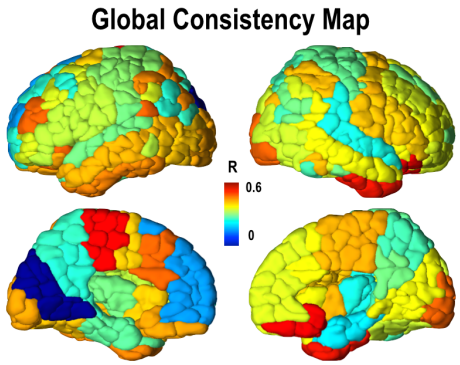

Figure 12. Consistency map of 38 modules

B. The dynamics of intra-module effective connectivity in lower level area and higher cognitive frontal area

After mapping the consistency (C) of 38 modules, we found characteristic local dynamics (Figure 10). Lower dynamicity in causal connectivity, which is equal to high consistency, was observed in primary visual cortex (module 7; C=0.4742) and secondary visual cortex (module 8; C=0.4623). The auditory cortex (module 5; C=0.4662) also showed high consistency, like the visual cortex (Figure 13A). Compared to the lower sensory areas, higher dynamics were observed in the higher cognitive frontal area (module 13; C=0.2854, module 14; C=0.3436) (Figure 13B).

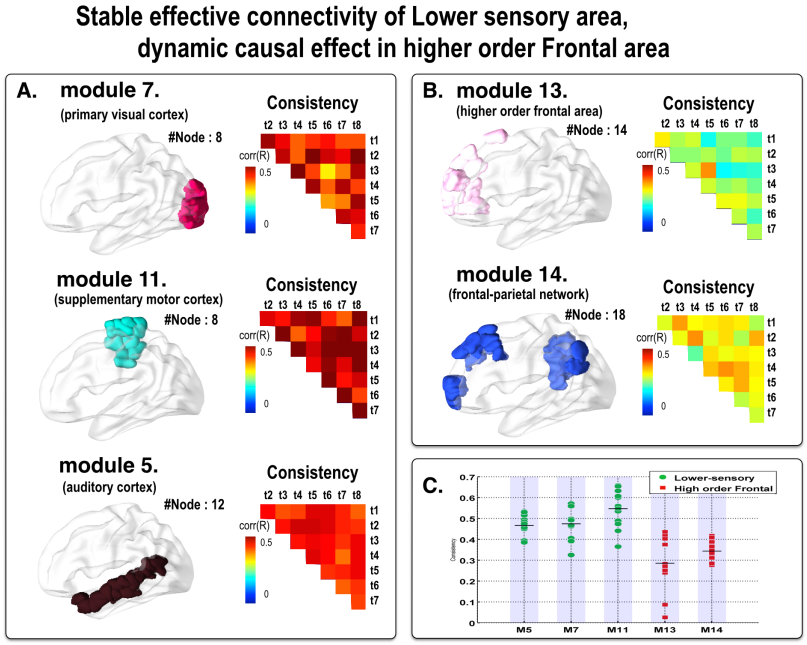

Figure 13. Comparison dynamicity between lower sensory area and high order frontal area

IV. DISCUSSION

Determining the dynamic components of spontaneous connectivity over the course of a day is important to clarify the function of the brain resting-state network. These dynamics can provide insights into the relationships between stationary brain network configuration, the characteristics of the flexible functional brain, and brain network organization altered by disease. Many studies have focused on the consistency of the default mode network across multiple sessions, subjects, and days in terms of spatial network patterns[41-43]. Recently, there has also been research on dynamic modular brain structure during learning and network dynamics during motor tasks[44, 45]. In this study, we examined the dynamic nodes, edges, and subnetworks in the resting state over a 24-hour period.

In contrast to the common assumption of a stable, long-term spontaneous resting-state network, the current results show the dynamicity of functional connectivity over 24 hours, which was reflected in ICC. We also observed highly dominant dynamic nodes through looking at their topological properties, and highly flexible nodes in the multilayer modular structure, which have an important role as hubs. Based on the assumption that the brain function is determined by its functional segregation locally and integration as a whole, we found dynamic subnetworks by looking at Graph ICA component weights.

Moreover, using directionality information and causal effects, we estimated

effective connectivity of the brain. We conducted stochastic DCM to determine the internal dynamic causal connectivity for the within-module effective connectivity of each subject and each time point. We examined the temporal consistency of among effective connectivity at 8 time points. High consistency in causal connectivity was observed in the primary visual cortex and secondary visual cortex. Additionally, the higher order frontal area showed greater dynamicity than the lower sensory areas. The results revealed that the dynamics of each subnetwork shows properties that are in accordance with the local function.

1. Characteristics of dynamic nodes

Within subnetworks, hubs exist to connect different nodes, resulting in small-world and scale-free properties[9-12]. Recent findings on human brain networks provide ample evidence that some brain regions may serve as hubs that are not responsible for a single function but are engaged in multiple cognitive functions. Thus, we investigated dynamic nodes and their relationship with hubs in order to understand diverse brain functionality.

According to previous research, local and global efficiency, as metrics for entire brain topology, show small-world properties in resting-state networks[46-48]. Global efficiency shows dynamicity, since it depends on a few randomly distributed long-range connections. Thus, the strength of these long-range

connections may be highly variable. In contrast, local efficiency, representing locally segregated connectivity, is consistent.

However, global properties present a limitation in explaining the role of each node. Thus, in this study, we applied ICC measurement and found the local properties to be dominantly dynamic. These dynamic node properties can be understood as dynamic functional connectivity because the topological properties are deeply related to the connection weights. The common dynamic nodes with regards to node strength, node efficiency and clustering coefficient (Figure 7) include the bilateral superior parietal gyri, right precuneus, left hippocampus, and lateral inferior parietal lobule. Furthermore, considering the multilayer modular structure of the brain, we looked at nodes whose module membership frequently changed. Nodes with significant values of nodal entropy were found in subcortical regions including the bilateral parahippocampal gyri, bilateral hippocampus, and bilateral superior frontal gyri (Figure 8).

The dynamic nodes we identified show similar composition to the rich club nodes discovered in previous research[12, 49]. Rich club nodes are “brain hubs”, that have a role in information integration and conferring robustness to structural core of brain. Rich club nodes are densely interconnected, shown through the construction of structural connectivity using diffusion tensor imaging data. Their similarity with the dynamic nodes of our study implies that the structurally high-degree nodes may be dynamically activated to manipulate

many functions. Compared to rich club nodes, putamen was not observed in either dynamic node properties or in flexible nodes in our study. Instead, in both cases, we found the bilateral inferior parietal lobules to be highly dynamic nodes.

2. Characters of dynamic and stable edges

We utilized ICC to measure the dynamicity of connection weights. The densities of dynamic edges were dominant (Figure 9). When we examined the stable connections, they were localized in each anatomical area, which indicates intra-region connections. The edges can be categorized as having short-range functional connectivity, showing segregated local structure that reflects the anatomical connectivity[50]. In contrast, long-range functional connectivity, which connects region to region (inter-region), would be more easily affected by cognitive control than by intrinsic short-range connectivity. Thus, dynamic global efficiency can be explained by the dynamic inter-region functional connections.

3. Features of dynamic subnetworks

The dynamic subnetworks identified by functional Graph ICA had two characteristics; intra-region subnetworks localized in the frontal area and inter-region subnetworks with long-range connectivity. We observed two independent components (IC2, IC41) that were comprised of bilateral superior

frontal gyri (dorsolateral, orbital part, and medial), bilateral middle frontal gyri, and bilateral inferior frontal gyri. These two components obviously represent components localized in the frontal area. Both IC64 and IC12 were long-ranged subnetworks. IC64 is a subnetwork connecting the frontal regions and occipital regions, while IC12 is a subnetwork that includes the subcortical regions of the bilateral inferior temporal gyri, middle temporal gyri, and cerebellum (Figure 10).

For within-module effective connectivity, higher-order frontal area show more dynamicity than lower sensory areas (Figure 13C). This is not surprising, as the frontal cortex supports higher-level cognitive skills (e.g., planning; reasoning; judgments; memory)[51] and completes the top-down modulation of sensory processing[52], both of which require dynamic processing functionality. Thus, our results show subnetwork dynamics that have properties in accordance with the local brain function.

V. CONCLUSION

In this study, to determine the dynamic elements in the resting-state fMRI network, we used multi-session data over the period of a day. We found dynamic nodes, edges and subnetworks using graph theory and novel methodology. The observed dynamic properties reflect the modular structure of brain and the functional integration. The brain network should be considered as a complex dynamic system that is temporally dynamic.

With the goal of predicting system behavior and designing perturbations to effect a specific outcome, it is crucial to find the relationships between the dynamic properties of the brain network and the functions of the brain. Using the network dynamics, we can explore the unknown aspects of brain connectivity, such as the hard-wired pathways and transient communication patterns inside the brain. Identifying organizational principles and developing novel diagnostics of disease are required in order to design personalized therapies and treatments for brain injury, neurological disease, and psychiatric disorders.

REFERENCES

1. Liu Y, Yu C, Liang M, Li J, Tian L, Zhou Y, et al. Whole brain functional connectivity in the early blind. Brain 2007;130(8):2085-96.

2. Sheline YI, Barch DM, Price JL, Rundle MM, Vaishnavi SN, Snyder AZ, et al. The default mode network and self-referential processes in depression. Proceedings of the National Academy of Sciences 2009;106(6):1942-7.

3. Gujar N, Yoo S-S, Hu P, Walker MP. The unrested resting brain: sleep deprivation alters activity within the default-mode network. Journal of cognitive neuroscience 2010;22(8):1637-48.

4. Anderson KJ, Revelle W. Impulsivity and time of day: Is rate of change in arousal a function of impulsivity? Journal of Personality and Social Psychology 1994;67(2):334.

5. May CP, Hasher L, Foong N. Implicit Memory, Age, and Time of Day Paradoxical Priming Effects. Psychological Science 2005;16(2):96-100.

6. Schmidt C, Collette F, Cajochen C, Peigneux P. A time to think: circadian rhythms in human cognition. Cognitive Neuropsychology 2007;24(7):755-89.

7. Gorfine T, Zisapel N. Late evening brain activation patterns and their relation to the internal biological time, melatonin, and homeostatic sleep debt. Human brain mapping 2009;30(2):541-52.

8. Park B, Kim JI, Lee D, Jeong SO, Lee JD, Park HJ. Are brain

networks stable during a 24-hour period? NeuroImage 2012;59(1):456-66.

9. Park H-J, Friston K. Structural and functional brain networks: from connections to cognition.; 2013. p. 1238411.

10. Bullmore ET, Bassett DS. Brain graphs: graphical models of the human brain connectome. Annual review of clinical psychology 2011;7:113-40.

11. Towlson EK, Vértes PE, Ahnert SE, Schafer WR, Bullmore ET. The rich club of the C. elegans neuronal connectome. J Neurosci; 2013. p. 6380-7.

12. van den Heuvel MP, Sporns O. Rich-club organization of the human connectome. J Neurosci; 2011. p. 15775-86.

13. Friston K. Dynamic causal modeling and Granger causality Comments on: the identification of interacting networks in the brain using fMRI: model selection, causality and deconvolution. NeuroImage; 2011. p. 303-5- author reply 10-1.

14. Friston KJ, Harrison L, Penny W. Dynamic causal modelling. NeuroImage; 2003. p. 1273-302.

15. Friston KJ, Li B, Daunizeau J, Stephan KE. Network discovery with DCM. NeuroImage; 2011. p. 1202-21.

16. Daunizeau J, Stephan KE, Friston KJ. Stochastic dynamic causal modelling of fMRI data: should we care about neural noise? NeuroImage; 2012. p. 464-81.

17. Li B, Daunizeau J, Stephan KE, Penny W, Hu D, Friston K.

Generalised filtering and stochastic DCM for fMRI. NeuroImage; 2011. p. 442-57.

18. Annett M. A classification of hand preference by association analysis. British journal of psychology 1970;61(3):303-21.

19. Friston KJ, Holmes AP, Worsley KJ, Poline JP, Frith CD, Frackowiak RSJ. Statistical parametric maps in functional imaging: A general linear approach. Human Brain Mapping 1994;2(4):189-210.

20. Tzourio-Mazoyer N, Landeau B, Papathanassiou D, Crivello F, Etard O, Delcroix N, et al. Automated anatomical labeling of activations in SPM using a macroscopic anatomical parcellation of the MNI MRI single-subject brain. NeuroImage 2002;15(1):273-89.

21. Park B, Ko JH, Lee JD, Park HJ. Evaluation of node-inhomogeneity effects on the functional brain network properties using an anatomy-constrained hierarchical brain parcellation. PloS one 2013;8(9):e74935.

22. Weissenbacher A, Kasess C, Gerstl F, Lanzenberger R, Moser E, Windischberger C. Correlations and anticorrelations in resting-state functional connectivity MRI: a quantitative comparison of preprocessing strategies. NeuroImage 2009;47(4):1408-16.

23. Thomas JB, Brier MR, Bateman RJ, Snyder AZ, Benzinger TL, Xiong C, et al. Functional connectivity in autosomal dominant and late-onset Alzheimer disease. JAMA neurology 2014;71(9):1111-22.

24. Taylor JS, Rastle K, Davis MH. Interpreting response time effects in functional imaging studies. NeuroImage 2014;99:419-33.

25. Muschelli J, Nebel MB, Caffo BS, Barber AD, Pekar JJ, Mostofsky SH. Reduction of motion-related artifacts in resting state fMRI using aCompCor. NeuroImage 2014;96:22-35.

26. Power JD, Barnes KA, Snyder AZ, Schlaggar BL, Petersen SE. Spurious but systematic correlations in functional connectivity MRI networks arise from subject motion. NeuroImage 2012;59(3):2142-54.

27. Van Dijk KR, Sabuncu MR, Buckner RL. The influence of head motion on intrinsic functional connectivity MRI. NeuroImage 2012;59(1):431-8.

28. Yan CG, Cheung B, Kelly C, Colcombe S, Craddock RC, Di Martino A, et al. A comprehensive assessment of regional variation in the impact of head micromovements on functional connectomics. NeuroImage 2013;76:183-201.

29. Genovese CR, Lazar NA, Nichols T. Thresholding of statistical maps in functional neuroimaging using the false discovery rate. NeuroImage 2002;15(4):870-8.

30. Rubinov M, Sporns O. Complex network measures of brain connectivity: uses and interpretations. NeuroImage 2010;52(3):1059-69.

31. Mucha PJ, Richardson T, Macon K, Porter MA, Onnela JP.

Community structure in time-dependent, multiscale, and multiplex networks. Science 2010;328(5980):876-8.

32. Traud AL, Kelsic ED, Mucha PJ, Porter MA. Comparing community structure to characteristics in online collegiate social networks. arXiv preprint arXiv:08090690 2008.

33. Rand WM. Objective criteria for the evaluation of clustering methods. Journal of the American Statistical association 1971;66(336):846-50.

34. Caceres A, Hall DL, Zelaya FO, Williams SC, Mehta MA. Measuring fMRI reliability with the intra-class correlation coefficient. NeuroImage 2009;45(3):758-68.

35. Deuker L, Bullmore ET, Smith M, Christensen S, Nathan PJ, Rockstroh B, et al. Reproducibility of graph metrics of human brain functional networks. NeuroImage 2009;47(4):1460-8.

36. Friedman L, Stern H, Brown GG, Mathalon DH, Turner J, Glover GH, et al. Test-retest and between-site reliability in a multicenter fMRI study. Hum Brain Mapp 2008;29(8):958-72.

37. Aron AR, Gluck MA, Poldrack RA. Long-term test-retest reliability of functional MRI in a classification learning task. NeuroImage 2006;29(3):1000-6.

38. Mazliak L, Shafer G. The splendors and miseries of martingales. Electronic Journal for History of Probability and Statistics Entire issue

dedicated to Martingale probability theory 2009;1(5).

39. Newman ME, Girvan M. Finding and evaluating community structure in networks. Physical review E, Statistical, nonlinear, and soft matter physics 2004;69(2 Pt 2):026113.

40. Newman ME. Finding community structure in networks using the eigenvectors of matrices. Physical review E, Statistical, nonlinear, and soft matter physics 2006;74(3 Pt 2):036104.

41. Chen S, Ross TJ, Zhan W, Myers CS, Chuang KS, Heishman SJ, et al. Group independent component analysis reveals consistent resting-state networks across multiple sessions. Brain research 2008;1239:141-51.

42. Damoiseaux JS, Beckmann CF, Arigita EJ, Barkhof F, Scheltens P, Stam CJ, et al. Reduced resting-state brain activity in the "default network" in normal aging. Cerebral cortex 2008;18(8):1856-64.

43. Meindl T, Teipel S, Elmouden R, Mueller S, Koch W, Dietrich O, et al. Test-retest reproducibility of the default-mode network in healthy individuals. Hum Brain Mapp 2010;31(2):237-46.

44. Bassett DS, Wymbs NF, Porter MA, Mucha PJ, Carlson JM, Grafton ST. Dynamic reconfiguration of human brain networks during learning. Proc Natl Acad Sci USA; 2011. p. 7641-6.

45. Bassett DS, Wymbs NF, Rombach MP, Porter MA, Mucha PJ, Grafton ST. Task-based core-periphery organization of human brain dynamics. PLoS

Comput Biol; 2013. p. e1003171.

46. Achard S, Bullmore E. Efficiency and cost of economical brain functional networks. PLoS computational biology 2007;3(2):e17.

47. Bassett DS, Bullmore E. Small-world brain networks. Neuroscientist; 2006. p. 512-23.

48. Sporns O, Zwi JD. The small world of the cerebral cortex. Neuroinformatics 2004;2(2):145-62.

49. Rubinov M, Bullmore E. Schizophrenia and abnormal brain network hubs. Dialogues Clin Neurosci; 2013. p. 339-49.

50. Honey CJ, Sporns O, Cammoun L, Gigandet X, Thiran JP, Meuli R, et al. Predicting human resting-state functional connectivity from structural connectivity. Proceedings of the National Academy of Sciences of the United States of America 2009;106(6):2035-40.

51. Badre D, Kayser AS, D'Esposito M. Frontal cortex and the discovery of abstract action rules. Neuron 2010;66(2):315-26.

52. Zhang S, Xu M, Kamigaki T, Hoang Do JP, Chang WC, Jenvay S, et al. Selective attention. Long-range and local circuits for top-down modulation of visual cortex processing. (1095-9203 (Electronic)).

ABSTRACT (IN KOREAN)

뇌 연결망에서의 동적인 노드, 연결성, 그리고 부분연결망

<지도교수 박 해 정>

연세대학교 대학원 의과학과

윤 미 선

최근 fMRI연구에서의 핵심은 뇌 연결성 연구라고 할 수 있다. 세계적인 연구 그룹들이 뇌 연결성을 이용하여 복잡계 시스템으로써 뇌를 이해하려고 노력하고 있다. 또한 뇌는 고정적인 해부학적 연결성(anatomical connectivity)을 가지고 있지만, 그 회로 위에서 다양한 뇌기능이 동작하도록 이루어져 있어, 그 기전을 외현활동 연결성(functional connectivity) 및 유효인과 연결성 (effective connectivity)를 통해 밝히려는 연구가 이루어지고 있다. 그러나, 기존의 뇌 연결성 연구들은 특정 시점에서 관심 영역내의 활성화 패턴만을 이용하는 것으로 제한되어 왔다. 본 연구에서는 뇌 연결망의 시간에 따른 역동성(dynamicity)을 측정하는 측도를 뇌영상 데이터에 맞게 개발하고 이를 적용하여 뇌에서 동적으로 변하는 연결망 요소, 예를 들어, 노드

(node), 연결 (edge), 부분연결망 (subnetwork)을 밝히고 그들이 뇌 기능에서 어떤 역할을 하는지 규명하였다. 또한, 뇌는 일반 네트워크 시스템과는 달리 동적인 시스템이므로, 시간에 따른 역동성을 측정하고 동역학적 모델로 뇌 기능을 설명해야 한다. 따라서 본 연구에서는 뇌 기능이 뇌의 국소적인 기능 분리와 총괄적인 기능 통합을 통해 이루어진다는 가설을 바탕으로, 뇌의 휴지기 인과적 연결성을 밝히는데에 뉴런 활동모델에 랜덤확률 변동을 고려한 stochastic DCM (sDCM)을 이용하여 내재적 동역학적 인과연결망을 추정하였다. 그 결과 낮은 계층의 감각처리 영역인 시각 피질 영역, 청각 피질 영역, 그리고 감각 운동영역이 인지기능을 담당하는 높은 계층의 전두엽 영역보다 더 낮은 역동성을 보이는 것을 관찰할 수 있었다. 따라서, 본 연구에서는 역동성을 지니는 요소들이 국소적으로는 각 영역의 기능과 상응하는 특성을 지니고, 전체적으로는 모듈 구조 통합 과정을 반영한다는 것을 보였다.

핵심되는 말 : 기능 자기공명영상, 휴지상태 외현활동 연결성, 그래프 이론, 부분연결망, 역동적 요소